Journal of MATERIALS RESEARCH

Article
DOI:10.1557/s43578-021-00230-5

3D PRINTING OF BIOMEDICAL MATERIALS AND DEVICES

FOCUS ISSUE

The effect of silk–gelatin bioink and TGF-β3 on mesenchymal stromal cells in 3D bioprinted chondrogenic constructs: A proteomic study

Shikha Chawla[1], Giovanna Desando[2], Elena Gabusi[3], Aarushi Sharma[1], Diego Trucco[3,4,5], Juhi Chakraborty[1], Cristina Manferdini[3], Mauro Petretta[2,6], Gina Lisignoli[3,a)], Sourabh Ghosh[1,a)]

[1] Regenerative Engineering Laboratory, Department of Textile and Fibre Engineering, Indian Institute of Technology, New Delhi 110016, India
[2] IRCCS Istituto Ortopedico Rizzoli, Laboratorio RAMSES, Bologna 40136, Italy
[3] IRCCS Istituto Ortopedico Rizzoli, Laboratorio di Immunoreumatologia e Rigenerazione Tissutale, Bologna 40136, Italy
[4] The BioRobotics Institute, Scuola Superiore Sant'Anna, Pisa, Italy
[5] Department of Excellence in Robotics & AI, Scuola Superiore Sant'Anna, 56127 Pisa, Italy
[6] RegenHU LTD, Z.I. Du Vivier 22, 1690 Villaz-St-Pierre, Switzerland
[a)] Address all correspondence to these authors. e-mails: gina.lisignoli@ior.it; Sourabh.Ghosh@textile.iitd.ac.in

Received: 27 February 2021; accepted: 28 April 2021

Sourabh Ghosh was an editor of this journal during the review and decision stage. For the JMR policy on review and publication of manuscripts authored by editors, please refer to http://www.mrs.org/editor-manuscripts/.

Major limitation of 3D bioprinting is the poor understanding of the role of bioink in modulating molecular signaling pathways. Phenotypically stable engineered articular cartilage was fabricated using silk fibroin–gelatin (SF-G) bioink and progenitor cells or mature articular chondrocytes. In the current study, role of SF-G bioink in modulating in vitro chondrogenic signaling pathways in human bone marrow-derived stromal cells (hMSCs) is elucidated. The interaction between SF-G bioink and hMSCs augmented several chondrogenic pathways, including Wnt, HIF-1, and Notch. We explored the debatable role of TGF-β signaling, by assessing the differential protein expression by hMSCs-laden bioprinted constructs in the presence and absence of TGF-β3. hMSCs-laden bioprinted constructs contained a large percentage of collagen type II and Filamin-B, typical to the native articular cartilage. Hypertrophy markers were not identified following TGF-β3 addition. This is first detailed proteomics analysis to identify articular cartilage-specific pathways in SF-G-based 3D bioprinted construct.

Introduction

Cartilage lesions have become a major health problem worldwide because of the limited regenerative capacity of articular cartilage following trauma or chronic joint disorders like osteoarthritis (OA) [1]. Despite multiple efforts in addressing this clinical need, there are no efficient and long-lasting therapies available for promoting cartilage regeneration [2]. Tissue engineering approaches, combining a range of biomaterials, cells, and growth factors, could provide prospecting alternatives [3–5]. Several unanswered questions and aspects of this technology remain to be elucidated to expand its clinical application. There is still a lack of understanding of the role of specific biomaterials in modulating molecular signaling pathways during *in vitro* chondrogenic differentiation.

In this direction, previously, we observed the alluring role of silk fibroin–gelatin (SF-G) bioink optimized by our group in developing 3D bioprinted cartilage and reducing hypertrophic processes [6–8]. The developed SF-G bioink and the optimized 3D bioprinting parameters allowed up to at least 80% cell viability of the encapsulated bone marrow-derived stromal cells (BMSCs) up to 40 days post-printing [7–9]. We deduced the probable role of SF-G-based bioink in hypoxia-mediated control

of hypertrophy, immobilization of growth factors, and control over canonical Wnt/β-catenin signaling [9], as observed from a limited set of gene and protein expression analysis. Therefore, in the present study, we aim to acquire a holistic view of the inherent regenerative potential of SF-G bioprinted constructs utilizing a scrupulous proteomics study enthralled on the key signaling pathways governing chondrogenesis.

Numerous studies have reported the effect of transforming growth factor-β (TGF-β) family members for controlling the composition, quality, and quantity of the secreted extracellular matrix (ECM) of progenitor cells in engineered cartilage constructs [10, 11]. In this light, our group showed the regulatory role of SF-G bioink on Wnt/β-catenin and Indian Hedgehog signaling pathways in driving hypertrophy throughout the chondrogenic differentiation of rat bone marrow-derived stromal cells (BMSCs) in the presence of TGF-β1 [8].

Interestingly, Haider *et al.* reported significantly increased deposition of chondrogenic ECM-like collagen type II and aggrecan in hMSCs-laden silk–elastin-like constructs in the presence of TGF-β3 [12]. Further, Li *et al.* reported that TGF-β3 could induce chondrogenic differentiation of adipose-derived stem cells by upregulating Wnt5a protein [13]. Although these studies shed light on the role of TGF-βs on chondrogenesis, there is still a limited and general grasp of the specific cellular signaling pathways. Therefore, the current study aimed to evaluate the impact of TGF-β3 in modulating chondrogenic differentiation of hMSCs encapsulated in 3D bioprinted SF-G constructs using extensive protein expression analysis. It elucidates the interactions among SF-G bioink and hMSCs in modulating chondrogenic signaling pathways in the control and chondrogenic groups cultured with and without TGF-β3 in the initial (day 1) and long-term culture (day 28). Then, we tried to elucidate the extent of ECM synthesis and remodeling by the hMSCs in the SF-G bioink's microenvironment in the control and chondrogenic groups at days 1 and 28. To date, this is the first study where the whole proteome analysis technique has been utilized to elucidate the protein expression related to cartilage-specific signaling pathways in a 3D bioprinted platform. This knowledge could provide essential insights in understanding how the bioprinted construct can create an active and instructive microenvironment for cells to promote cartilage-specific tissue regeneration.

Results

Cell Viability

Following the post-printing process, the microscopic analysis of constructs evidenced a homogeneous cell distribution (Figure 1a). The cells remained homogenously distributed till day 28 (Figure 1b). About 95% of cells were viable (green cells)

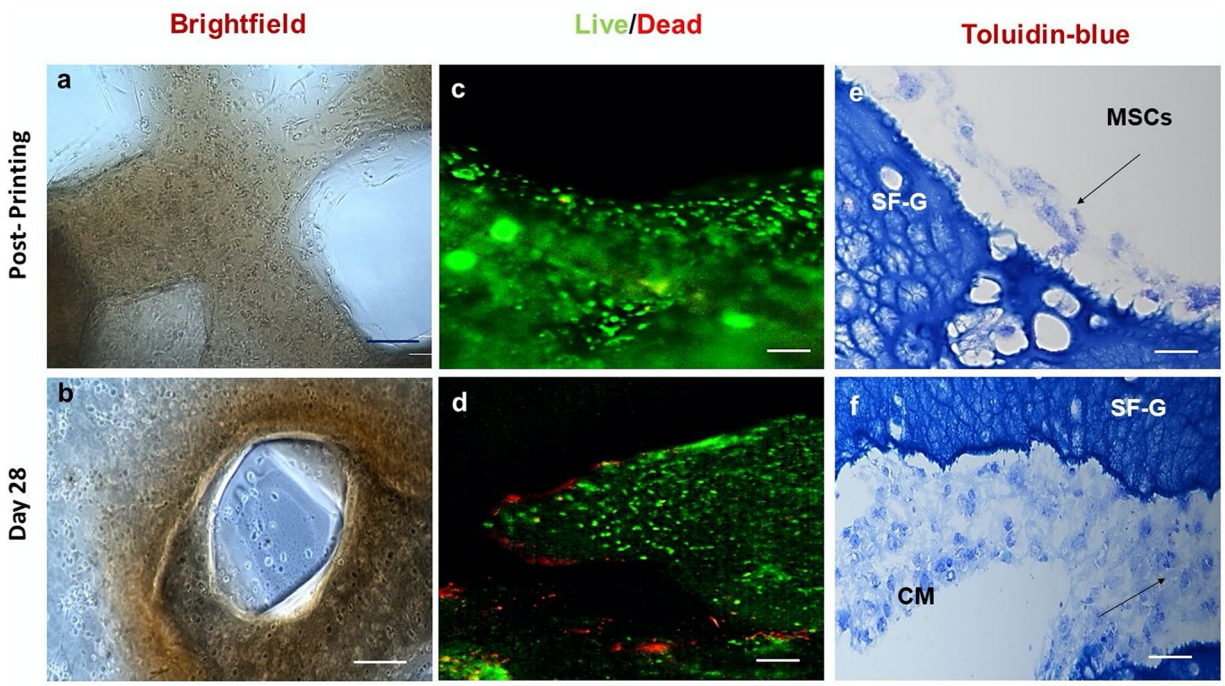

Figure 1: Representative micrographs of 3D SF-G constructs post-printing and chondrogenic group at day 28. Bright-field images of 3D SF-G construct (a). post-printing and (b). the chondrogenic group captured with the inverted microscope (scale bar: 100 μm). Live and dead images of 3D SF-G constructs (a) post-printing and (b). chondrogenic group (scale bar: 50 μm), green: live cells; red: dead cells. Toluidine blue staining of 3D SF-G constructs (a). post-printing and (b) chondrogenic group (scale bar: 50 μm), *CM* the presence of cartilage matrix, *SF* silk–fibroin matrix, *MSC* mesenchymal stromal cells.

post-printing, whereas only a low percentage of cells (about 5%) (red cells) were dead (Figure 1c). An optimal viability ratio (about 90%) of cells was also observed on day 28 (Figure 1d), as we reported earlier [8, 9]. Toluidine blue staining gave evidence of the neo-ECM formation [14] in the chondrogenic group at day 28 (Figure 1f). The control group (post-printing) showed merely a few cells dispersed along the edges of the SF-G hydrogel (Figure 1e). Nevertheless, because of the strong affinity of the SF-G hydrogel for Toluidine blue dye, it was feasible to visualize many cells and ECM deposition within the printed hydrogel filament structures and peripheral parts of the constructs.

Proteomics analyses

Gene ontological analysis

PANTHER categorized the total genes corresponding to the protein list in the control group (days 1 and 28), and the chondrogenic group (day 28) into GO term Biological Processes. Identified proteins expressed as early as day 1 showed association with the in vivo like GO terms, GO Developmental process and GO Signaling (Figure S1). Additionally, for all the time points PANTHER analysis revealed the association of the identified proteins with critical GO Cellular processes like cell growth, cell cycle, cell division, cellular development processes, signal transduction, cell communication, cell metabolic processes as well as actin filament-based processes at all the time points (Figure S1-S3).

TABLE 1: List of genes analyzed using qRT-PCR.

Gene name	Full from	Cat. no.
GAPDH	Glyceraldehyde-3- phosphate-dehydrogenase	QT00079247
SOX9	SRY-Box Transcription Factor 9	QT00001498
COL2A1	Collagen type II alpha 1 chain	QT00049518
ACAN	Aggrecan	QT00001365
COMP1	Cartilage oligomeric matrix protein 1	QT00001050
COL1A1	Collagen type I alpha 1 chain	QT00037793
COL10A1	Collagen type X alpha 1 chain	QT00096348
TGFβR1	TGF beta receptor 1	QT00083412
ITGAX	Integrin Subunit Alpha X	QT00030646
CDH1	Cadherin 1	QT00080143

KEGG pathway analysis by DAVID

KEGG pathway analysis performed using DAVID revealed several chondrogenic signaling pathways in the control group at day 1 (Supplementary Table 1). The differentially expressed proteins in the control and chondrogenic groups at day 28 categorized under KEGG pathways showed that both groups shared a few common chondrogenic pathways (Table 2). We observed a pro-chondrogenic behavior of the SF-G bioink even in the absence of exogenously added TGF-β3. Interestingly, the chondrogenic group displayed an upregulated expression of the TGF-β signaling pathway, thereby indicating a direct role of TGF-β3 in inducing TGF-β signaling. Conversely, the control group exhibited a downregulated expression of the TGF-β signaling pathway.

PANTHER pathway analysis

According to cartilage catabolic and anabolic pathways, PANTHER pathway analysis arranged the list of upregulated and downregulated proteins in the day 28 control and chondrogenic groups compared to the day 1 control group, as mentioned in

TABLE 2: KEGG pathway analysis in the control and chondrogenic group (day 28 vs day 1) as identified by DAVID.

Day 28 Control (no TGF-β3) group	Day 28 Chondrogenic (with TGF-β3) group	Day 28 both Control and Chondrogenic group
KEGG pathways corresponding to upregulated proteins (day 28 vs day 1)		
Glycosaminoglycan biosynthesis-chondroitin sulfate/dermatan sulfate	TGF-β signaling pathway	MAPK signaling pathway
		PI3K-Akt signaling pathway
		Rap1 signaling pathway
		mTOR signaling pathway
		Regulation of actin cytoskeleton
		FoxO signaling pathway
		Hippo signaling pathway
		Wnt signaling pathway
		Notch signaling pathway
		HIF-1 signaling pathway
		Signaling pathways regulating pluripotency of stem cells
KEGG pathways corresponding to downregulated proteins (day 28 vs day 1)		
TGF-β signaling pathway	–	Oxytocin signaling pathway
		NF-kappa B signaling pathway
		Jak-STAT signaling pathway

Table 3 (Figure S4–S7). For a better understanding, we have categorized the PANTHER analysis results under various pathways by explaining the role of a few critical proteins implicated in chondrogenic differentiation and cartilage development.

Wnt signaling pathway Proteins related to the Wnt signaling pathway were expressed in both control and chondrogenic groups at day 28 (Table 3). However, there were differences concerning the list of upregulated or downregulated proteins corresponding to different Wnt signaling like canonical Wnt/β-catenin signaling, Wnt/planar cell polarity (Wnt/PCP) pathway, and Wnt/calcium pathway. For instance, the overexpression of β-catenin, frizzled receptors, and Actin in the control group indicated activation of canonical Wnt/β-catenin signaling [14–16]; simultaneously, the upregulation of Cadherin-related family member 2 (CDHR2) indicated toward a feedback mechanism possibly inhibiting canonical Wnt/β-catenin signaling [17]. Moreover, the upregulated expression of Protocadherin and Cadherin EGF LAG seven-pass G-type receptor 3 (CELSR3) in the presence of TGF-β3 indicated the activation of Wnt/PCP pathway and control of chondrocyte phenotype in the presence of through regulation of actin cytoskeleton. CELSR3 3 is involved with the control of planar cell polarity during embryonic spinal cord development [18, 19]. The overexpression of 1-phosphatidylinositol 4,5-bisphosphate phosphodiesterase beta-3 and 4 was indicative of the presence of Wnt/Ca^{2+} signaling [20]. The downregulation of several protocadherins indicated the downregulation of the Wnt/PCP pathway [19]. Additionally, downregulation of SWItch/sucrose non-fermentable (SWI/SNF) complex unit indicated reduced nuclear translocation of β-catenin since SWI/SNF complex has

TABLE 3: Signaling pathways corresponding to differentially expressed proteins at day 28 control (no TGF-β3) and chondrogenic groups (with TGF-β3) at day 28 as compared to day 1 control group.

Overexpressed proteins		Underexpressed proteins	
Control group Day 28	Chondrogenic group Day 28	Control group Day 28	Chondrogenic group Day 28
Wnt signaling pathway			
1-phosphatidylinositol 4,5-Bisphosphate phosphodiesterase beta-3	Protocadherin-19	Protocadherin-1	Protocadherin-1
Actin, Aortic smooth muscle	Inositol 1,4,5-triphosphate	Protocadherin gamma-B3	
Cadherin-related family member 2	Protocadherin-9	Protocadherin gamma-A3	
Actin, cytoplasmic 1	Cadherin EGF LAG seven-pass G-type receptor 3	Protocadherin gamma-A2	
Frizzled-9	SWI/SNF complex unit	Protocadherin gamma-A7	
Catenin β-1	Adenomatous polyposis coli protein	SWI/SNF complex unit	
Frizzled-5		Alpha-catulin	
1-phosphatidylinositol 4,5-Bisphosphate phosphodiesterase beta-2			
Integrin signaling pathway			
Engulfment and cell motility protein 1	Engulfment and cell motility protein 1	Integrin alpha-V	
Fibronectin	Filamin-B	Integrin beta-2	
Laminin subunit	Talin-1	Ras-related protein Rap-1b-like protein	
Talin-1			Not detected
Collagen alpha-1(XXVII) chain COL27A1			
TGF beta signaling pathway			
Inhibin beta E chain	Growth/differentiation factor 6	Growth/differentiation factor 6	Not detected
	Mothers against decapentaplegic homolog 7		
Notch signaling pathway			
Disintegrin and metalloprotease domain-containing protein 10	Disintegrin and metalloprotease domain-containing protein 10	Not detected	Not detected
Nuclear receptor corepressor	Gamma secretase subunit APH-18		
Notch 1	Notch 1		
p38 MAPK pathway			
Mitogen-activated protein kinase kinase kinase 10	Not detected	Not detected	Not detected

been reported to enhance the nuclear accumulation of β-catenin in the Wnt/β-catenin signaling pathway [21].

The list of upregulated proteins corresponding to the Wnt/β-catenin signaling pathway in the day 28 chondrogenic group included (SWI/SNF) complex, which suggested increased nuclear translocation of β-catenin since as explained above SWI/SNF complex is described to augment the nuclear accumulation of β-catenin [21]. Remarkably, the upregulation of adenomatous polyposis coli (APC) protein that acts downstream of Wnt/β-catenin signaling provided substantial evidence of the active Wnt/β-catenin signaling. Further, there was upregulation of Wnt/PCP pathway-specific Protocadherin-19 and Protocadherin-9 that play a significant role during actin assembly, cell polarity, and morphogenesis [19].

Integrin signaling pathway On day 28, the control group overexpressed proteins (Table 3) included engulfment and cell motility protein 1 (ELMO1) that is related to activation of RHO/RAC GTPases [22]. There was also upregulation of collagen alpha-1(XXVII) chain (COL27A1) involved in cartilage calcification [23]. Further, there was upregulation of fibronectin, laminin subunit, and Talin-1 cartilage ECM components that interact with integrins [24]. The list of downregulated proteins in the control group included Integrin alpha-V, one of the main integrins of articular cartilage [24] other proteins related to cellular adhesion. In the chondrogenic group, the list of upregulated proteins included ELMO-1 and Talin-1 similar to control; further, the overexpression of Filamin-B (FLNb) was unique to the chondrogenic group at day 28.

Notch signaling pathway Both control and chondrogenic groups displayed overexpression of Notch 1 in (Table 3) at day 28, which is an essential modulator of Notch signaling and a critical regulator in cartilage development [25]. The chondrogenic group showed an upregulation of Notch signaling downstream protein gamma-secretase subunit APH-18, thus providing further evidence of an active Notch signaling in the presence of TGF-β3.

TGF-β signaling pathway The most exciting observation related to identifying the TGF-β signaling pathway was the downregulation of growth differentiation factor-6 (GDF6) in the control group, while GDF6 was upregulated in the chondrogenic group (Table 3). The chondrogenic group showed an upregulation of mother against decapentaplegic homolog 7 (SMAD7) that can inhibit both BMP and TGF-β pathways [26].

Expression of collagens and associated cartilage-specific ECM components

To assess the extent of expression of cartilage-specific ECM components in the SF-G bioprinted constructs, the list of identified proteins was assessed for the presence of collagens and associated proteins, MMPs and GAGs in the control group at days 1 and 28 and chondrogenic group on day 28 (Table 4). The most interesting observation was the expression of procollagen-lysine, 2-oxoglutarate 5-dioxygenase 1 (PLOD-1) at day 1, involved with the hydroxylation of lysyl residues during biosynthesis of collagen biosynthesis. On day 1, the control group overexpressed procollagen galactosyltransferase 1 (COLGALT1), capable of transferring galactose to hydroxylysine residues of collagens I-V [27]. There was an expression of COLXI that helps in the adjustments of the length of the ECM fibers [28]. It is important to mention here that previous studies on BMSC-seeded transwell constructs have demonstrated the significance of COLII and COLXI crosslinks in maintaining the robustness of the developed neocartilage [29]. There was also an expression of COLIV and COLX1V that regulates fibrillogenesis [30]. Expression of COLI is reported in early condensed mesenchymal bodies during *in vitro* chondrogenic differentiation of MSCs in pellet culture [31]. On day 28 in the control group, there was a continued expression of COLGALT1 and COLIV. Additionally, there was an expression of COLXIV and COLXXIV involved in mature cartilage matrix formation [32]. On day 28, the chondrogenic group displayed COLIV, COLXI, and COLXIV, all related to articular cartilage as explained earlier. Interestingly, there was an expression of COLVI that is reported to increase the differentiation of MSCs toward cartilage-like phenotype during *in vitro* pellet culture [33]. Further, no proteins related to calcified hypertrophic cartilage were detected in the chondrogenic group. At both time points, the control group expressed matrix metalloproteinase-16 (MMP-16), which is overexpressed in the end stage of OA in cartilage [34]. In the chondrogenic group, there was an expression of MMP-20 with no mentioned expression in articular cartilage. We observed the expression of chondroitin sulfate, a major ECM GAG component, and Beta-1,4-galactosyltransferase 7 at all the time points. Interestingly, the expression of dermatan sulfate epimerase another ECM GAG was observed only in the control group (both day 1 and day 28) (Table 4).

Gene expression analyses

Real-time RT-PCR was performed to assess gene expression changes of chondrogenic markers, *SOX9*, *COL2A1*, *ACAN*, and *COMP1* at days 14 and 28 (Figure 2). The control group displayed nominal gene expression (less than onefold change) of *SOX9* at both time points, whereas the chondrogenic group showed a 2.5- and 4.5-fold increase on days 14 and 28. The chondrogenic group displayed a four- and ninefold increase of *SOX9* compared to the control group at days 14 and 28 (**$P < 0.01$; ***$P < 0.0001$, respectively) (Figure 2a). The *COL2A1* expression followed a similar trend with negligible expression levels at both time points for the control group, whereas the chondrogenic group displayed a 2.5- and 18.5-fold increase at days 14 and 28,

TABLE 4: Major ECM components synthesized by hMSCs in the control group at day 1 and day 28 and chondrogenic group at day 28.

Control Group Day 1			Control group Day 28			Chondrogenic group Day 28		
Accession	Gene	Protein	Accession	Gene	Protein	Accession	Gene	Protein
Collagens								
Q02809	PLOD1	Procollagen-lysine,2-oxoglutarate 5-dioxygenase 1	P53420	COL4A4	Collagen alpha-4(IV) chain	P08572	COL4A2	Collagen alpha-2(IV) chain
P08572	COL4A2	Collagen alpha-2(IV) chain	Q8NBJ5	COLGALT1	Procollagen galactosyltransferase 1	Q01955	COL4A3	Collagen alpha-3(IV) chain
Q8NBJ5	COLGALT1	Procollagen galactosyltransferase 1	Q96P44	COL21A1	Collagen alpha-1(XXI) chain	P13942	COL11A2	Collagen alpha-2(XI) chain
P13942	COL11A2	Collagen alpha-2(XI) chain	Q2UY09	COL28A1	Collagen alpha-1(XXVIII) chain	P12110	COL6A2	Collagen alpha-2(VI) chain
Q14031	COL4A6	Collagen alpha-6(IV)	Q05707	COL14A1	Collagen alpha-1(XIV)	A6NMZ7	COL6A6	Collagen alpha-6(VI) chain
Q05707	COL14A1	Collagen alpha-1(XIV) chain	Q17RW2	COL24A1	Collagen alpha-1(XXIV)	Q96P44	COL21A1	Collagen alpha-1(XXI) chain
P02452	COL1A1	Collagen alpha-1(I)				Q05707	COL14A1	Collagen alpha-1(XIV) chain
P39060	COL18A1	Collagen alpha-1(XVIII) chain						
MMPs								
P51512	MMP16	Matrix metalloproteinase-16	P51512	MMP16	Matrix metalloproteinase-16	O60882	MMP20	Matrix metalloproteinase-20
GAGs								
Q8N6G5	CSGALNACT2	Chondroitin sulfate N-acetylgalactosaminyltransferase 2	Q8IZ52	CHPF	Chondroitin sulfate synthase 2	Q8IZ52	CHPF	Chondroitin sulfate synthase 2
Q9UBV7	B4GALT7	Beta-1,4-galactosyltransferase 7	Q9UBV7	B4GALT7	Beta-1,4-galactosyltransferase 7	Q9UBV7	B4GALT7	Beta-1,4-galactosyltransferase 7
Q9UL01	DSE	Dermatan sulfate epimerase	Q9UL01	DSE	Dermatan sulfate epimerase			

respectively. The chondrogenic group showed a 4- and a 37-fold increase for *COL2A1* when compared to the control at 14 and 28 days, respectively (**P < 0.01 and ***P < 0.0001, respectively) (Figure 2b). The gene expression levels of cartilage ECM components like *COMP1* and *ACAN* were also assessed. The control group showed negligible levels of both *COMP1* and *ACAN* at day 14. *COMP1* followed a similar trend as *COL2A1*, where the chondrogenic group showed a 15.5- and 27-fold increase at days 14 and 28. As for *COMP1*, the chondrogenic group revealed a 32- and 54-fold increase for *COMP1* compared to the control at both 14 and 28 days (***P < 0.0001) (Figure 2c). As for *ACAN*, the chondrogenic group showed an eightfold increase on day 14 and a 5.5-fold decrease on day 28. The comparison of both day 14 and day 28 expression levels of *ACAN* revealed a 15- and 11-fold upregulated expression in the chondrogenic group as compared to the control group (***P < 0.0001) (Figure 2d). The control group showed 0.6-fold expression of *COL1A1* at day 14 that increased to tenfold at day 28 (Figure 2e). The chondrogenic group showed negligible expression (less than onefold) of *COL1A1* at both day 14 and day 28 (Figure 2e). We further assessed the gene expression levels of cartilage hypertrophic gene *COL10A1* by finding a threefold upregulated expression at day 14 for the control group, which increased to 15-fold on day 28. The comparison of both day 14 and day 28 expression levels of *COL10A1* revealed a six- and 30-fold downregulated expression in the chondrogenic group compared to the control group (**P < 0.01 and ***P < 0.0001, respectively) (Figure 2f).

Additionally, we assessed the expression of a few of the pathway-specific genes like TGF-β pathway-specific *TGFβR1*, Integrin pathway-specific *ITGAx,* and Cadherin pathway-specific *CDH1* (Figure 3). All three genes *TGFβR1*, *ITGAx,* and *CDH1* showed a similar profile with negligible expression levels at both day 14 and day 28 in the control group. Furthermore, *TGFβR1* showed a stable expression pattern at both day 14 and day 28 for the chondrogenic group. The comparison of day 14 expression levels of *TGFβR1* revealed a twofold upregulated expression in the chondrogenic as compared to the control group (**P < 0.01) (Figure 3a). The control group showed a negligible expression of *ITGAx* at both 14 and 28 days. Furthermore, the expression of *ITGAx* showed a negligible expression at day 14 for the chondrogenic group that increased to 2.2-fold on day 28. The comparison of day 28 expression levels of *ITGAx* revealed a 2.2-fold upregulated expression in the chondrogenic as compared to the control

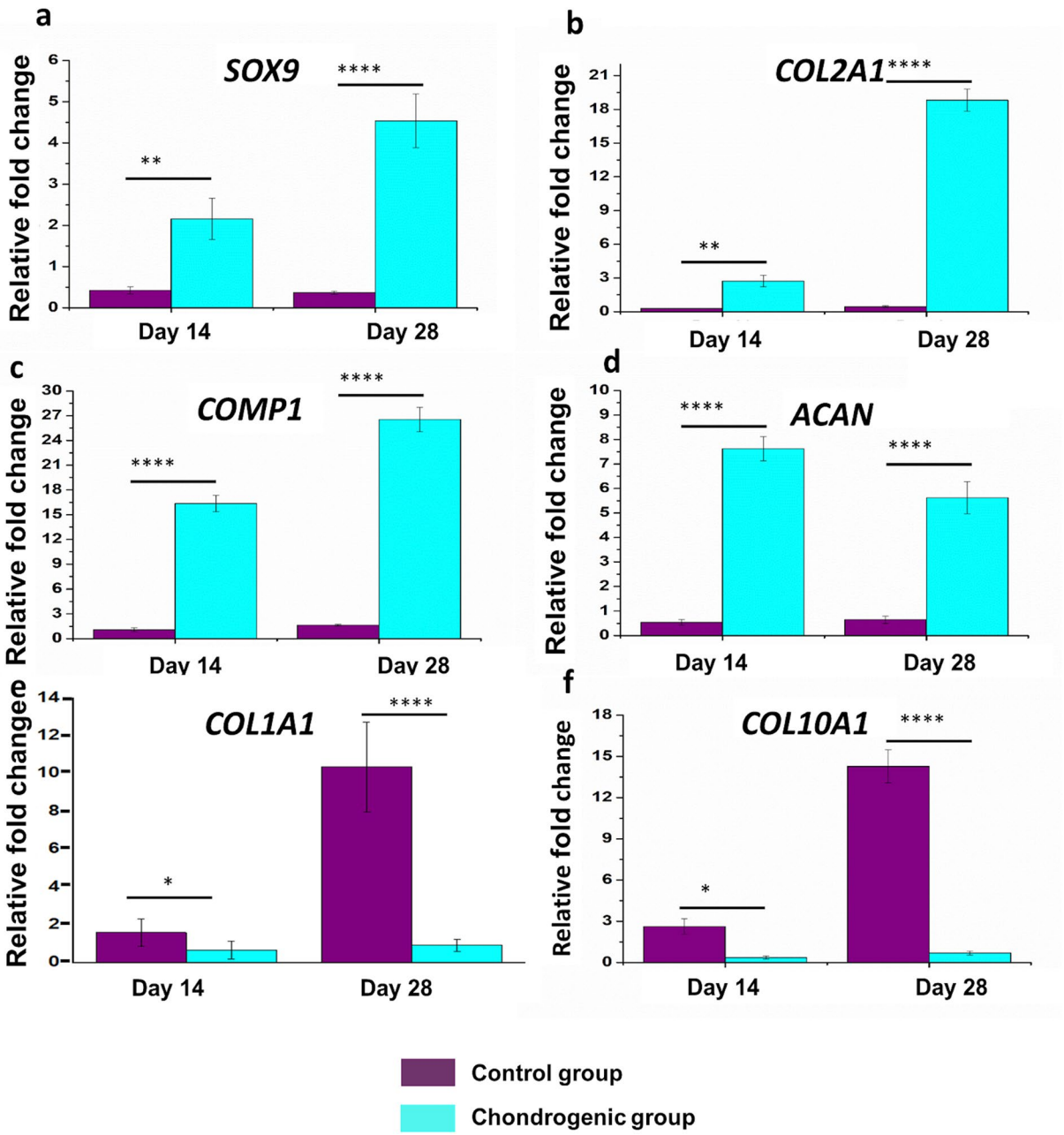

Figure 2: qRT-PCR-based gene expression analysis depicting the expression of chondrogenic markers *(SOX9, COL2A1, ACAN, and COMP1)*, de-differentiation marker (*COL1A1*), and hypertrophic cartilage marker (*COL10A1*) in the control and chondrogenic group. The relative fold changes in the expression levels were calculated using the $2^{-(\Delta\Delta c(t))}$ method, using monolayer hMSCs at day 0 (cultured in the absence of chondrogenic factors) as controls. *P < 0.05, **P < 0.01, ***P < 0.001, and ****P < 0.0001 were considered significant (control vs chondrogenic group at day 14 and day 28).

group (***P < 0.0001) (Figure 3b). The control group showed a negligible expression of *CDH1* at both day 14 and 28 days. Furthermore, the expression of *CDH1* showed 2.5-fold upregulated expression at day 14 for the chondrogenic group that increased to fourfold on day 28. The comparison of days 14 and 28 expression levels of CDH*1* revealed a 2.5- and fivefold upregulated expression in the chondrogenic as compared to the control group (**P < 0.01 and ***P < 0.001, respectively) (Figure 3c).

Immunohistochemical analyses

Immunohistochemical analyses further confirmed the articular cartilage-specific chondrogenic differentiation of bioprinted constructs (Figure 4). As shown in Figure 4, we evidenced at day 28 that the chondrogenic markers, collagen type 2 (Figure 4a-c) and aggrecan (Figure 4d-f), were positive only in the chondrogenic group (Figure 4b-c and Figure 4e-f, respectively), mainly evident on the cells but also on the construct that assumed a

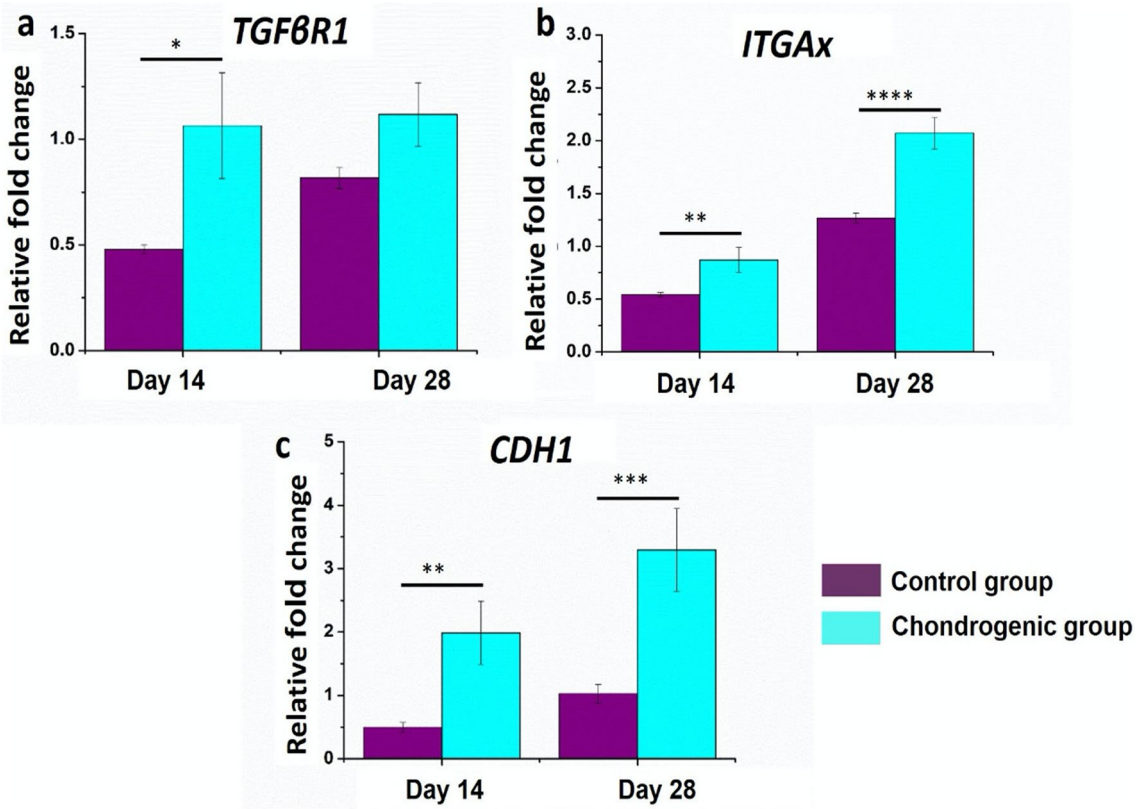

Figure 3: qRT-PCR-based gene expression analysis depicting the expression of cartilage-specific pathway markers (*TGFβR1, ITGAx,* and *CDH1*). *P < 0.05, **P < 0.01, ***P < 0.001, and ****P < 0.0001 were considered significant (control vs chondrogenic group at day 14 and day 28).

mixed color between red (positive area) and blue (hematoxylin counterstained area). The inclusion of negative and relative isotype-matched controls confirmed the positivity for collagen type 2 and aggrecan specifically found only on chondrogenic differentiated hMSCs encapsulated in 3D bioprinted SF-G construct. Interestingly, collagen type 1 was negative in both control (Figure 4g) and the chondrogenic group (Figure 4h-i). Moreover, to confirm the results obtained with monoclonal anti-collagen type 1, positive control of osteogenic differentiated hMSCs laden in 3D SF-G [35] was also checked.

Discussion

3D bioprinting attempts to develop tissue-engineered constructs that can closely mimic the architectural and biological characteristics of native cartilage. However, most of the current studies in this direction do not focus on assessing detailed molecular signaling pathways that would aid in developing phenotypically stable articular cartilage. Our earlier studies on 3D bioprinting for cartilage repair exquisitely highlighted modulation of HIF1 and canonical Wnt/β-catenin signaling pathways following the interaction of SF-G bioink with progenitor cells [7, 8, 36]; however, we could not provide proof of concept for the modulation of these signaling pathways at the protein level. In this light, we aimed to deepen this analysis by providing a detailed picture of the molecular signaling pathways modulating chondrogenic differentiation of hMSCs in bioprinted SF-G constructs to understand the intrinsic regenerative potential of the bioink.

3D bioprinted SF-G was able to modulate the anabolic and catabolic chondrogenic signaling pathways of hMSCs encapsulated under both control and chondrogenic culture conditions. Interestingly, the observation of the GO term "Developmental process" highlighted the role of SF-G bioink in augmenting the expression of proteins related to *in vivo* development processes by providing a microenvironment favoring the differentiation of hMSCs.

Further, the KEGG pathway analysis provided an initial view of the signaling pathways activated upon the interaction of SF-G bioink and encapsulated hMSCs. The presence of cell adhesion molecules (CAMs) that are significant during the MSC condensation [37] and ECM–receptor interaction gave further evidence of an *in vivo*-like 3D microenvironment promoting chondrogenic responses. The signaling pathway related to glycosaminoglycan biosynthesis-chondroitin sulfate/dermatan sulfate (Table 2) further substantiated the positive interaction between SF-G bioink and hMSCs in promoting a cartilage-specific microenvironment [38].

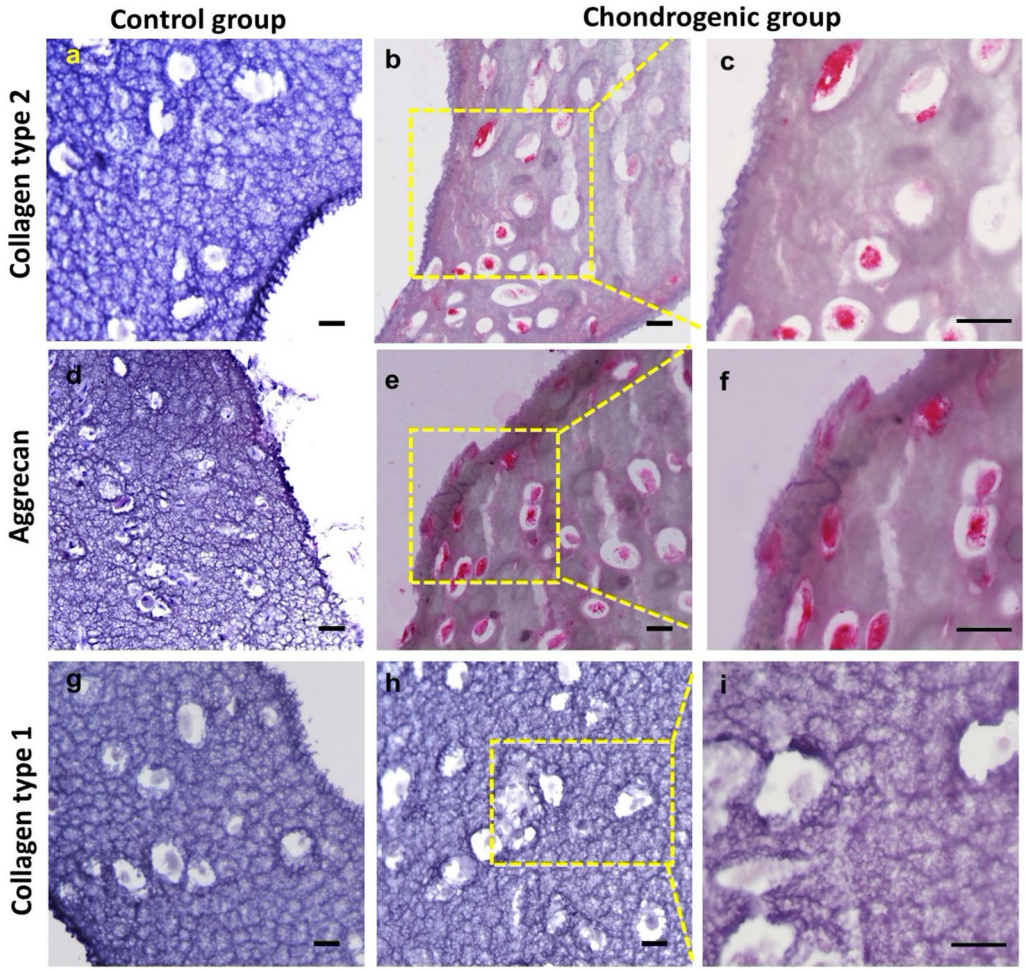

Figure 4: Immunohistochemical analysis of collagen type 2, aggrecan, and collagen type 1 at day 28 of hMSCs embedded in 3D SF-G hydrogel constructs in both control and chondrogenic groups. Scale bar = 100 μm.

The activation of cartilage-specific major anabolic signaling pathways like Wnt, Notch, and HIF-1 signaling pathways interestingly indicated a promising interaction between SF-G bioink and hMSCs [7, 8, 10, 39]. Wnt signaling governs the stable articular cartilage-like differentiation of mesenchymal progenitor cells during cartilage development [40]. Notch signaling is another key regulator in cartilage development and joint maintenance, and its loss results in early and progressive OA-like pathology [25]. HIF-1 signaling also plays a significant role during chondrogenesis through two oxygen-sensitive transcription factors: hypoxia-inducible factor-1 and -2 alpha (HIF-1α and HIF-2α). HIF-1α improves chondrogenesis of MSCs by interacting with the SOX9 promoter and suppresses hypertrophy through Runx2 inhibition [41]. We can conclude that even the initial interaction between SF-G bioink and hMSCs was enough to launch *in vivo* chondrogenically relevant cellular signaling pathways.

Further studies were addressed to understand the modulation of these initial signaling pathways till day 28. Herein, the KEGG pathway analysis (Table 2) showed an increased chondrogenic profile of hMSCs embedded in SF-G bioink. The expression of Wnt, TGF-β, Integrin, and HIF-1 signaling pathways indicated toward the expression of *in vivo* like signaling pathways by hMSCs in the presence of SF-G matrix (Table 2) [42]. These findings corroborated with the gene expression results and with our previous studies [7, 8]. The PANTHER analyses provided a detailed picture of differential protein expression-based pathway at day 28 compared to day 1 in the control group (Table 3).

Interestingly, no downstream component of canonical Wnt/β-catenin signaling was expressed in the control group (Table 3). These observations indicated the possibility of canonical Wnt/β-catenin signaling to promote transient hypertrophic cartilage-like differentiation of hMSCs. Extended Notch 1 overexpression in the control group even at day 28 stipulated Notch signaling's involvement as modulated by the SF-G matrix. The downregulation of TGF-β signaling pathway-specific GDF6 in the chondrogenic group at day 28 (Table 3) could correspond

to the overexpression of hypertrophic marker *COLX* that marks the initiation of ossification. GDF6 plays a role in suppressing ossification during the development of spinal columns [43, 44]. During culture time progression, there were upregulation and a feedback loop-based downregulation of Wnt/β-catenin via activation Wnt/Ca^{2+} signaling which possibly led to the hypertrophic differentiation of hMSCs in the control group. Nevertheless, there was upregulation of other critical cartilage-specific signaling pathways like HIF-1, Notch, glycosaminoglycan biosynthesis-chondroitin sulfate/dermatan sulfate that highlighted the regenerative potential of the SF-G bioink in inducing cartilage tissue-specific differentiation of hMSCs.

Next, we examined the proteins expressed in the control and chondrogenic group for the collagen associated proteome as well as other ECM and their regulatory roles to understand the regenerative potential of the SF-G matrix at the early time point and under the influence of long-term culture till 28 days (Table 4). The identification of PLOD-1 and COLGALT1 at day 1 implied normal collagen synthesis and post-translational modifications (PTM) essential for generating stable articular cartilage *in vitro.* These proteins play a significant role during collagen biosynthesis *in vivo* [27]. The expression of COL IV at day 1 and continued expression till day 28 was also significant to our study since COLIV has been reported to play a role in maintaining the hypoxic microenvironment in articular cartilage [45]. This observation correlates well with the observed expression of HIF-1a in our previous study, where we speculated the role of SF-G bioink in regulating hypoxic microenvironment similar to *in vivo* articular cartilage [7]. Apart from the fact that there was articular-specific COLXIV expression, the expression of COLXXIV and COLXXVII (that have been related to bone matrix and calcified cartilage, respectively [46, 47]) indicated toward hypertrophic cartilage-like differentiation of hMSCs at day 28 in the control condition as corroborated with the gene expression results.

PANTHER analysis also indicated toward the expression of cartilage-specific ECM proteins fibronectin, laminin, Talin-1 [24] and the involvement of active integrin signaling till later time point of day 28 (Table 3) accentuating the role of our SF-G matrix in inducing cartilage-specific ECM synthesis. The downregulation of the main integrin component of cartilage, Integrin alpha-V, indicated toward downregulation of cartilage-specific integrin proteins synthesis at day 28 [24]. The observed downregulation of Integrin alpha-V could be anticipated for the observed underexpression of chondrogenic markers as observed from the gene expression analysis. Therefore, the SF-G bioink modulated the chondrogenic differentiation of hMSCs leading to cartilage-specific ECM synthesis.

Further, we tried to utilize the extensive proteomics analysis to understand how cells can remodel their surrounding SF-G bioink matrix during culture. Matrix metalloproteinases play a significant role in remodeling cartilage tissue [7]. The observed expression of MMP-16 on day 1 and its extended expression till day 28 in control conditions implied several levels of matrix remodeling. MMP-16 synthesis has been reported in human osteoarthritic cartilage; thus, the remodeling occurring in our constructs was speculated to be degradative [34]. Moreover, we observed an upregulation of ELMO protein, a critical regulator of Rac signaling [22]. In articular chondrocytes, Rac signaling acts by accelerating the rate of chondrogenic differentiation by increasing COLX promoter activity [39]. Thus, overexpression of ELMO1 as late as day 28 of chondrogenic differentiation could be one of the factors responsible for the overexpression of hypertrophic marker *COLX* further indicating hypertrophic cartilage-like differentiation in the control group.

Next, we aimed to assess the beneficial effect of inclusion of TGF-β3 during the culture in modulating the interaction of hMSCs with the SF-G bioink on the chondrogenic signaling pathways, ECM deposition, and matrix remodeling. TGF-β proteins are among the main molecules used for promoting chondrogenic differentiation of progenitor cells; however, the literature is ambiguous about their role. *In vivo* in healthy cartilage tissue, TGF-β signaling initiates via TGF-β type I receptor (TGFβR1/ALK5) and Smad2/3 to provoke anabolic signaling. Loss of this signal is associated with the degradation of cartilage [48]. TGF-β3 has also been reported to inhibit terminal differentiation of chondrocytes during *in vitro* differentiation of hMSCs [49, 50]. On the other hand, transient TGF-β1 induces activation of TGF-β signaling in the hMSCs of the subchondral bone or synovial layer, leading to OA-like features [51]. Thus, in the current study, we attempted to explore the impact of TGF-β3 on hMSCs-laden 3D SF-G constructs by evaluating several catabolic and anabolic cartilage-specific signaling pathways.

The upregulation of APC in the presence of TGF-β3 provided additional substantiation of active canonical Wnt/β-catenin signaling in the bioprinted constructs [52]. Further, the expression of CELSR3 indicated embryonic level regulation of the Wnt/PCP pathway in the presence of TGF-β3 instead of the bioprinted constructs cultured in the absence of TGF-β3. All the same, the identification of SWI/SNF complex in the upregulated group of proteins identified in the bioprinted constructs in the presence of TGF-β3 indicating toward increased protein levels of β-catenin and its enhanced nuclear accumulation providing evidence for the prevalence of active canonical Wnt/β-catenin signaling in the presence of TGF-β3 [21, 53]. The upregulation of Notch signaling downstream protein γ-secretase in the presence of TGF-β3 furnished additional proof for active Notch signaling on the addition of TGF-β3. In a study, where hMSCs were cultured in monolayer, inhibition of Notch signaling with the γ-secretase inhibitor DAPT leads to inhibited proliferation and chondrogenic differentiation of hMSCs [54]. The upregulation of GDF6 on the addition of TGF-β3 could be the reason

for the suppression of hypertrophy and expression of chondrogenic markers in the chondrogenic group. Further, in the case of TGF-β3, there was an upregulation of SMAD7, which has been reported to inhibit both BMP and TGFβ pathways [26, 55]. For articular cartilage-like stable chondrogenic differentiation, we need control over BMP signaling [56]. Thus, the overexpression of SMAD7 could be responsible for keeping a check over BMP signaling that is a key factor leading to hypertrophic terminal differentiation of chondrocytes [26]. These results corroborate with the gene expression results of TGFBR1 another member of the TGF-β family, where overexpression of TGFBR1 was observed in the presence of TGF-β3 probably mediating effects similar to SMAD7 in counteracting the BMP signaling pathway. The evaluation of the ECM synthesis reported all the collagens related to *in vivo* healthy articular cartilage and no expression of hypertrophic markers. Further, there was an expression of Collagen VI that has also been reported to bind the chondrocytes to the matrix [28]. The synthesis of Collagen VI in our bioprinted constructs is an indicator of positive modulation of the hMSCs by SF-G bioink toward chondrogenic protein expression in the presence of TGF-β3. These data imply that there is a control over hypertrophic differentiation in the presence of TGF-β3.

Furthermore, the overexpression of FLNb was unique to the bioprinted constructs on the addition of TGF-β3. The loss of FLNb has been reported to cause the premature differentiation of chondrocytes into the pre-hypertrophic chondrocytes [57]. Thus, overexpression of FLNb on the addition of TGF-β3 could be one of the reasons for enhanced chondrogenic differentiation in the presence of TGF-β3.

While evaluating the modulation of matrix remodeling on the inclusion of TGF-β3, we observed overexpression of ELMO1 similar to the control group. Herein, it is essential to mention the negative modulation of chondrogenic differentiation asserted by ELMO1, which might be counteracted by other integrin family members. *ITGAx* could suppress the tendency of hypertrophic differentiation noticed in the chondrogenic group, cultured with TGF-β3.

Further, the gene expression analysis was used to assess the chondrogenic differentiation potential of the hMSCs-laden 3D bioprinted SF-G constructs. This analysis indicated that the hMSCs-laden 3D SF-G constructs treated with TGF-β3 showed higher expression of articular cartilage markers *SOX-9*, *COL2A1*, *ACAN,* and *COMP1* than the control group. The IHC expression of collagen type II and aggrecan only in the chondrogenic group further substantiated this observation. The chondrogenic group also displayed low gene expression for *COL10A1*, typically promoting hypertrophic responses. The most interesting finding in the chondrogenic group was the overexpression of *TGFβR1/ALK5* a canonical type I receptor for TGFβs activating Smads2/3 in human cartilage [58].

Conversely, the control group showed downregulation of *TGFBR1* by indicating hypertrophic cartilage-like differentiation of hMSCs. I*n vitro* knockdown of ALK5 fosters terminal hypertrophic differentiation of chondrocytes [58]. Beyond its role in hypertrophy, TGFBR1 modulates BMP by blocking the ACVRL1-mediated BMP signaling [59]. Thus, we can speculate that the overexpression of *TGFBR1* (significant at day 14 and not significant at day 28) in TGF-β3-treated hMSC encapsulated SF-G constructs probably played two roles, by mediating the TGF-β pathway-mediated articular cartilage differentiation. The upregulation of *ITGAx* in the chondrogenic group at both day 14 and day 28 would indicate the inhibition of hypertrophic phenotype by TGF-β3. It is well known that *ITGAx* binds to collagen type II by *in vivo* suppressing hypertrophic differentiation [60].

Mass spectrometry-based cartilage proteome profiling approaches have been used in the past to generate insights into mechanisms of cartilage degeneration *in vitro* and *in vivo* [61]. Schneider *et al.* utilized ECM characterization produced by chondrocytes encapsulated in PEG hydrogels to assess the variation of the secretome as a function of hydrogel stiffness and culture condition [62]. They reported the secretion of many collagen-rich proteins and biglycan preserved independently of culture environments of the hydrogel. However, they did not study the role of different pathways and proteins in the expression of hypertrophic markers, which are essential for developing stable articular cartilage *in vitro*. Gardner *et al.* [63] tried to identify the differences in the secretome of hMSCs induced toward chondrogenesis through the application of chondrogenic differentiation factor TGF-β and mechanical load. They studied a set of 174 proteins and identified differences in the levels of latency-associated peptide and leptin in the two experimental groups. Further, using quantitative proteomics Wang *et al.* demonstrated the increased expression of COMP neo-epitopes as potential biomarkers of OA in mechanical injury-related human knee explants [64]. However, in all these studies, the authors did not deduce detailed interaction between the molecular signaling pathways leading to the observed results.

Several attempts have been made to study the differences in the proteome profiling of healthy and osteoarthritic cartilage [65]. But this is the first study reporting such extensive proteome profiling of the *in vitro* silk-based bioprinted constructs to identify articular cartilage-specific signaling pathways in 3D bioprinted tissue-engineered cartilage constructs. Further, unlike the studies mentioned above, our study successfully identified the expression of *in vivo* like chondrogenic signaling pathways like Wnt/β-catenin, Wnt/PCP, HIF-1, Notch, and signaling, thus highlighting the regenerative potential of SF-G-based bioinks. We understand that this is a pilot study and we considered only a single concentration of TGF-β3 supplemented twice a week as a part of chondrogenic differentiation media with our SF-G

bioink. Future studies are still necessary to better elucidate the role of several gradients and time intervals of TGF-β3 within such hydrogel-based bioink in modulating chondrogenesis pathways. Moreover, while we could comprehend several critical unanswered aspects of *in vitro* chondrogenic differentiation in SF-G bioink-based 3D bioprinted constructs, we understand that extensive western blot-based validation of the proteins of interest would be needed.

Conclusion

We have reported inherent regenerative potential of SF-G bioink as it induced activation of the Wnt/β-catenin signaling pathway in hMSCs [36]. However, there were indications for both activation and inhibition of Wnt/β-catenin signaling, probably leading to the observed expression of hypertrophic cartilage markers. SF-G bioink promoted several anabolic chondrogenic signaling pathways (Notch, HIF-1, integrin signaling pathways) and inhibited catabolic pathways NF-κB signaling during culture.

We further tried to shed light on the ambiguous role of TGF-β signaling *in vitro*, as modulated by SF-G bioink in the presence and absence of TGF-β3. The addition of TGF-β3 promoted chondrogenic differentiation and controlled hypertrophic phenotype by activating the Wnt/β-catenin signaling. Further, our results successfully showed the activation of the TGF-β signaling pathway following the addition of TGF-β3, by demonstrating its role in inducing stable chondrogenic differentiation at both gene and protein levels. We could identify several members of the TGF-β signaling pathways like GDF6 and TGFβR1 that have been reported to counteract the effects of BMP signaling and thus playing a role in controlling the hypertrophic differentiation of cultured hMSCs.

Materials and methods

Silk fibroin extraction

The *Bombyx mori* cocoons were provided by the Central Silk Technological Research Institute (Central Silk Board, Bangalore, Ministry of Textiles, Government of India). We followed the extraction protocol already published to obtain the SF solution from *Bombyx mori* cocoons [66, 67]. Briefly, 2.5 gm of cocoons was cut with scissors and boiled twice into 0.02 M sodium bicarbonate (Sigma-Aldrich) for 20 min and then washed in distilled water to remove sericin. The fibers were dried at 37°C overnight and then dissolved in 9.3 M lithium bromide (LiBr, Sigma-Aldrich) solution for 4 h at 60°C. To remove LiBr, the SF solution was dialyzed with deionized water at room temperature (RT) for 48 h and then stored at 4°C. Protein percentage determination of the SF solution was performed as previously described [35, 68].

Bioink preparation

The bioink was prepared by adding Gelatin (G, ~ 300 g Bloom, Sigma-Aldrich) (5% w/v) to the SF solution (5% w/v). Briefly, to obtain a final volume of 1.5 mL of bioink, 1.2 mL of SF solution and 75 mg of G powder from porcine skin type A (Sigma-Aldrich) were mixed. The solution was incubated in a thermostatic bath at 37°C for 30 min. Then, 150 µL of Dulbecco's modified Eagle's (DMEM, 10X) high glucose medium (Euroclone) and 150 µL of fetal bovine serum (FBS, 10%) (Euroclone) were added. Finally, 21.5 µL of mushroom tyrosinase enzyme (Sigma-Aldrich) (430 U/1.5 mL) was added to the bioink to initiate crosslinking.

Cell encapsulation and bioprinting

Human bone marrow was harvested from an anonymous healthy donor to isolate human mesenchymal stromal cells (hMSCs) (with institute ethics committee approval, IRCCS Istituto Ortopedico Rizzoli [69]), and biological triplicates were considered for the isolation. A total of 1×10^7 cells hMSCs at passage 3 were encapsulated per mL of SF-G-based bioink, immediately after the addition of 430 U of tyrosinase (Sigma-Aldrich) under laminar flow at RT. hMSCs-laden SF-G bioink was gently loaded into the cartridge and closed by piston and needle in sterile conditions [35].

The cartridge was then mounted on the pressure-based direct dispensing printhead of the 3D Discovery Bioprinting platform (RegenHU). The bioprinting process started 20 min after the tyrosinase addition to allow a suitable initial degree of reticulation. 6 x 6 mm (length x width) Constructs were printed using an internal pattern based on parallel lines at alternating angles of 0° and 90° with an inter-filament distance of 1.2 mm in both directions (x and y) to guarantee open and interconnected pores. The printing needle was 6.35 mm long, with a diameter of 0.2 mm. The optimal printing parameters were, $P = 1.2 \times 10^5$ Pa, $v = 1.5$ mm/s and at a printing temperature of 18 ± 2 °C. The final 3D structure was composed of 10 layers, featuring an overall thickness of 1.2 mm.

Cell culture and chondrogenic differentiation

hMSCs-laden 3D SF-G constructs were kept at RT for 20-30 min after the printing and then transferred in non-adherent 24 wells (Corning Inc). Constructs were cultured with the basal chondrogenic medium DMEM High Glucose supplemented with ITS (6.25 µg/mL of insulin, 6.25 µg/mL of transferrin, 6.25 ng/mL di selenium) (Sigma-Aldrich), premix (5.33 µg/mL of linoleic acid, 1.25 mg of bovine serum albumin), 0.1 µM dexamethasone (Sigma-Aldrich), 37.5 µg/mL ascorbic acid (Sigma-Aldrich),

1 mM sodium pyruvate (Sigma-Aldrich), 100 U/mL penicillin (Sigma-Aldrich), and 100 µg/mL streptomycin (Sigma-Aldrich). After 48 h, the culture medium was replaced, maintaining half of the constructs in basal chondrogenic medium (namely control group) and the other half in the chondrogenic differentiation medium that is a basal chondrogenic medium containing 10 ng/mL TGF-β3 to (namely chondrogenic group). The 3D SF-G constructs were analyzed on days 1, 14, and 28. The culture medium was changed twice a week. Bright-field microscopic images of the constructs were captured post-printing and at day 28 using the microscope (Nikon, Eclipse 90i) to evaluate cell distribution and integrity of the constructs. Cell viability, gene expression, protein expression, and immunohistochemical analyses were carried out.

Cell viability

We assessed the cell viability of SF-G constructs (chondrogenic group) immediately after bioprinting and at the established endpoints (day 14 and day 28) by Live and Dead assay (Thermo Fisher Scientific). Constructs were washed with phosphate-buffered saline (PBS, Sigma-Aldrich) and then incubated with ethidium homodimer-1 (4 µM) and calcein-AM (2 µM) for 45 min. We visualized labeled cells with the Eclipse 90i microscope with fluorescein isothiocyanate (FITC) and tetramethylrhodamine (TRITC) filters (Nikon, Japan) for evaluating viable (green) and dead/necrotic (red) cells [8]. Percentage cell viability was calculated from the microscopic images using ImageJ (NIH, USA) [8]. At the designed experimental times, constructs were embedded with optimal cutting temperature (OCT) and snap-frozen in liquid nitrogen. After cryostat cutting, sections were stained with 1% Toluidine blue solution (Sigma-Aldrich) for 5 min at RT, followed by rinsing steps with deionized water. Slides were dried at RT, and later sections were covered with a coverslip using an aqueous mounting medium. Sections were examined under a light microscope (Nikon, Eclipse 90i).

Proteomic analyses

Protein extraction from hMSC-laden 3D bioprinted SF-G constructs

hMSCs-laden 3D SF-G constructs were collected at day 1 (control group) and day 28 (control and chondrogenic groups) and were treated with 100 µl of lysis buffer (Tris–HCl-NaCl-Nonidet P-40-S DS, sodium fluoride (1 mM, Sigma-Aldrich), sodium orthovanadate (1 mM, Sigma-Aldrich), phenylmethylsulfonyl fluoride (1 mM, Sigma-Aldrich), protease inhibitor cocktail (Sigma-Aldrich, diluted 1:200) and quickly snap-frozen in liquid nitrogen. Samples were incubated in lysis buffer for 15 min and then centrifuged at 7000 X g at 4°C for 15 min. Supernatants were collected, and Pierce BCA Protein Assay kit (Thermo Fisher Scientific) was used to quantify the extracted proteins according to manufacturer protocol and stored at −80°C.

In-solution trypsin digestion

The elution of co-immunoprecipitated proteins was done in 30 µl elution buffer (50 mM Glycine, pH 2.8). 25 µg of eluted protein from each sample was used for in-solution trypsin digestion (Promega). The samples were incubated at 37°C for 10 min while shaking. Samples were treated with 200 mM dithiothreitol (Sigma-Aldrich) in 50 mM ammonium bicarbonate (Sigma-Aldrich) (final concentration of 10 mM iodoacetamide) and heated at 75° C for 15 min; the samples were then allowed to cool and spun down. Samples were incubated with 200 mM iodoacetamide (Sigma-Aldrich) in 50 mM ammonium bicarbonate (final concentration of 50 mM iodoacetamide) in the dark for 30 min. The samples were incubated with trypsin (1:50, trypsin: protein) overnight at 37°C. 0.5% w/v trifluoroacetic acid (Sigma-Aldrich) and 2% w/v acetonitrile (Sigma-Aldrich) were added to the samples followed by incubation at RT for 5 min, and the samples were spun down for 10 min followed by desalting and peptides using C18 spin columns (Thermo) [70]. The digested samples were finally dried using a speed vacuum concentrator (Thermo Savant DNA 120) before MS.

Mass spectrometry analyses

The digested samples were analyzed with a Nano1200 chromatography system (Thermo Scientific) attached to the QExactive orbitrap mass spectrometer (Thermo Scientific) that is equipped with a nano-electrospray ion source. The dried pellet was resuspended in Buffer A (0.1% formic acid in water), and 1 µg was loaded onto a 50 cm x 75 µm long EASY-Spray column (PepMap RSLC) packed with 2 µm-C18 resin. The peptides were eluted in 5-40% gradient of buffer B (100% acetonitrile, 0.1% formic acid) for 102 mins, 40-90% gradient of buffer B for 1 min, and finally in 90% gradient of buffer B for 15 min at a flow rate set at 300 ml/min and a total run time of 123 min. The MS data were acquired using a data-dependent acquisition method choosing 10 most intense peaks with charge state +2 to +5 in positive polarity with exclude isotope option enabled and a dynamic exclusion time of 12 sec. The maximum limit of ions or full scan target for MS1 was 3 x 10^6 within a time of 60 msec, and the mass range was set between 350 and 2000, while the target value for MS2 was set at 1 x 10^5 with an intensity threshold set at 8.3 x 10^2. The isolation window of parent ions was set at 1.5 m/z, normalized collision energy for higher-energy collisional dissociation (HCD) was set at 27, peptide match option set to preferred mode and isotope exclusion mode enabled. Both MS1 and MS2 scans were acquired with a resolution of 70,000 and 17500 at m/z 200-2000, respectively [71].

Data search and protein identification

Raw data files acquired from the orbitrap mass spectrometer were processed by MaxQuant 1.5.2.8, and relative protein abundance for different proteins was compared [72]. The peptides were identified (label-free quantification, trypsin enzyme with one missed cleavage) against the SwissProt database (Homosapien's taxonomy) downloaded from UniProt in December 2019 (with MaxQuant's database of internal contaminants).

Data annotation

The identified protein list was searched for the expression of articular cartilage-specific ECM proteins at all the time points. Further, the identified protein list was sorted for upregulated and downregulated proteins at day 28 in the control and chondrogenic group and compared to the control group on day 1. The sorting was done based on the abundance ratio. Proteins with an abundance ratio greater than 1 were grouped as upregulated, and those less than 1 were grouped as downregulated. Entrez Ids corresponding to individual proteins expressed in the control group at days 1 and 28 and the chondrogenic group day 28 were first used for Gene Ontological (GO) analysis using Protein ANalysis THrough Evolutionary Relationships (PANTHER) assigning them to various GO terms. The overexpressed and underexpressed proteins were further used for pathway analysis with PANTHER. We also applied the Database for Annotation, Visualization, and Integrated Discovery (DAVID) bioinformatics tools, specifically interrogating gene representation in the Kyoto Encyclopedia of Genes and Genomes (KEGG) pathway database.

Gene expression analyses

3D SF-G constructs from the control, and chondrogenic groups were collected at days 1, 14, and 28 in 1.5 mL tubes with 1 mL of EuroGold RNAPure™ (Euroclone, Milano), immediately snap-frozen in liquid nitrogen and stored at -80°C. According to the manufacturer's protocol, total RNA was extracted using a pestle for fragmentation of the constructs to allow better cell lysis. Total RNA was reverse-transcribed into cDNA using the first-strand cDNA Super Script® Vilo™ cDNA synthesis Kit (Invitrogen). Real-time PCR was carried out with SYBR Green Master Mix and Rotor gene Q thermocycler (Qiagen). To this end, we used Quantitect primers (Qiagen), chondrogenic (*SOX9*, *COL2A1*, *ACAN*, and *COMP1*), de-differentiation (*COL1A1*), hypertrophic (*COL10A1*), and cartilage-specific pathway (*TGFβR1*, *ITGAx,* and *CDH1*) markers, where *GAPDH* was used as a housekeeping gene (Table 1). The analysis was carried out using the Rotor gene Q software, and the relative fold changes in the expression levels were calculated using the $2^{-(\Delta\Delta c(t))}$ method, using monolayer hMSCs at day 1 (cultured in the absence of chondrogenic factors) as controls.

Immunohistochemical analyses

3D SF-G constructs were embedded in optimal cutting temperature (OCT) compound (Kaltek Srl) and snap-frozen in liquid nitrogen. Twelve-µm-thick sections were cut, air-dried, and stored at −20 °C until their immunohistochemical staining. Briefly, the slides were kept at RT, air-dried for 20 min, and fixed in 10% formaldehyde (Kaltek Srl) for 1 h. Then, samples were re-hydrated with Tris-buffered saline (TBS, Sigma-Aldrich), and the non-specific antigenic sites were blocked with a Protein Block Serum-Free (Dako) for 10 min at RT. Then, sections were incubated for 1 h at RT with monoclonal mouse anti-human collagen type 2 (diluted 1:20), cartilage proteoglycan aggrecan (diluted 1:20), and anti-collagen type 1 (diluted 1:50) antibodies (all from Chemicon International) diluted with TBS. After 3 washing steps in PBS, sections were firstly incubated with multi-linked biotinylated secondary antibody and then with the alkaline phosphatase-conjugated streptavidin (Biocare Medical) at RT for 10 min, respectively. The colorimetric reactions were developed using a Fast red kit (Biocare Medical), and the nuclear component was counterstained with CAT hematoxylin. The sections were evaluated under a bright-field microscope (Nikon, Eclipse 90i). Specifically, negative and isotype-matched control sections were performed.

Statistical Analyses

Statistical analyses were performed using GraphPad Prism 8 software (San Diego). One-way ANOVA followed by Bonferroni multiple comparison tests was used. *$P < 0.05$, **$P < 0.01$, ***$P < 0.001$, and ****$P < 0.0001$ were considered significant. Data were represented as the mean ± standard deviation (SD). All the experiments were performed in triplicates, with biological experiments carried out in triplicates [35].

Funding

This work was jointly funded by the Department of Science and Technology, India, and the Italian Ministry of Foreign Affairs and International Cooperation. This work was partially supported by Istituto Ortopedico Rizzoli funds: "5 per mille and ricerca corrente".

Declaration

Conflict of interest The authors declare no conflict of interest.

Supplementary Information

The online version contains supplementary material available at https://doi.org/10.1557/s43578-021-00230-5.

References

1. R.S. Tiğli, S. Ghosh, M.M. Laha, N.K. Shevde, L. Daheron, J. Gimble, M. Gümüşderelioğlu, D.L. Kaplan, Comparative chondrogenesis of human cell sources in 3D scaffolds. J. Tissue Eng. Regen. Med. **3**, 348–360 (2009)
2. M. Bhattacharjee, J. Coburn, M. Centola, S. Murab, A. Barbero, D.L. Kaplan, I. Martin, S. Ghosh, Adv. Drug Deliv. Rev. **84**, 107–122 (2015)
3. K. Dzobo, N.E. Thomford, D.A. Senthebane, H. Shipanga, A. Rowe, C. Dandara, M. Pillay, K.S.C.M. Motaung, Advances in regenerative medicine and tissue engineering: Innovation and transformation of medicine. Stem Cells Int. **2018**, 24 (2018)
4. L. Roseti, C. Cavallo, G. Desando, V. Parisi, M. Petretta, I. Bartolotti, B. Grigolo, Materials (Basel). **11**(9), 1749 (2018)
5. G. Cidonio, M. Glinka, J.I. Dawson, R.O.C. Oreffo, Biomaterials **209**, 10–24 (2019)
6. S. Das, F. Pati, Y.J. Choi, G. Rijal, J.H. Shim, S.W. Kim, A.R. Ray, D.W. Cho, S. Ghosh, Bioprintable, cell-laden silk fibroin-gelatin hydrogel supporting multilineage differentiation of stem cells for fabrication of three-dimensional tissue constructs. Acta Biomater. **11**, 233–246 (2015)
7. S. Chameettachal, S. Midha, S. Ghosh, Regulation of chondrogenesis and hypertrophy in silk fibroin-gelatin-based 3D bioprinted constructs. ACS Biomater. Sci. Eng. **2**(9), 1450–1463 (2016)
8. S. Chawla, A. Kumar, P. Admane, A. Bandyopadhyay, S. Ghosh, Elucidating role of silk-gelatin bioink to recapitulate articular cartilage differentiation in 3D bioprinted constructs. Bioprinting. **7**, 1–13 (2017)
9. S. Chawla, A. Sharma, A. Bandyopadhyay, S. Ghosh, Developmental biology-inspired strategies to engineer 3D bioprinted bone construct. ACS Biomater. Sci. Eng. **4**(10), 3545–3560 (2018)
10. O.T. Quen, K. Shakib, M. Heliotis, E. Tsiridis, A. Mantalaris, U. Ripamonti, E. Tsiridis, TGF-beta3: a potential biological therapy for enhancing chondrogenesis. Expert Opin. Biol. Ther. **9**(6), 689–701 (2009)
11. H. Madry, A. Rey-Rico, J.K. Venkatesan, B. Johnstone, M. Cucchiarini, Transforming growth factor beta-releasing scaffolds for cartilage tissue engineering. Tissue Eng. Part B Rev. **20**(2), 106–125 (2014)
12. M. Haider, J. Cappello, H. Ghandehari, K.W. Leong, In vitro chondrogenesis of mesenchymal stem cells in recombinant silk-elastinlike hydrogels. Pharm. Res. **25**, 692 (2008)
13. D. Li, X. Ma, T. Zhao, Mechanism of TGF-β3 promoting chondrogenesis in human fat stem cells. Biochem. Biophys. Res. Commun. **530**(4), 725–731 (2020)
14. N.L. Bergholt, H. Lysdahl, M. Lind, C.B. Foldager, A standardized method of applying toluidine blue metachromatic staining for assessment of chondrogenesis. Cartilage **10**(3), 370 (2019)
15. S. Chawla, A. Sharma, A. Bandyopadhyay, S. Ghosh, Developmental biology-inspired strategies to engineer 3D bioprinted bone construct. ACS Biomater. Sci. Eng. **4**(10), 3545–3560 (2018)
16. K.A. Staines, V.E. Macrae, C. Farquharson, Cartilage development and degeneration: a Wnt Wnt situation. Cell Biochem. Funct. **30**(80), 633–642 (2012)
17. R. Ose, T. Yanagawa, S. Ikeda, O. Ohara, H. Koga, PCDH24-induced contact inhibition involves downregulation of β-catenin signaling. Mol. Oncol. **3**(1), 54–66 (2009)
18. X.-J. Wang, D.-L. Zhang, Z.-G. Xu, M.-L. Ma, W.-B. Wang, L.-L. Li, X.-L. Han, Y. Huo, X. Yu, J.-P. Sun, Understanding CELSRs-Cadherin EGF LAG seven-pass G-type receptors NIH public access. J. Neurochem. **131**(6), 699–711 (2014)
19. K.M. Mah, J.A. Weiner, Expanding functions of ADP-ribosylation in the maintenance of genome integrity. Semin. Cell Dev. Biol. **69**, 158–171 (2017)
20. E. Sandsmark, A.F. Hansen, K.M. Selnæs, H. Bertilsson, A.M. Bofin, A.J. Wright, T. Viset, E. Richardsen, F. Drabløs, T.F. Bathen, M.B. Tessem, M.B. Rye, A novel non-canonical Wnt signature for prostate cancer aggressiveness. Oncotarget **8**(6), 9572–9586 (2017)
21. Y. Wang, J. Qin, Q. Liu, X. Hong, T. Li, Y. Zhu, L. He, B. Zheng, M. Li, SNF2H promotes hepatocellular carcinoma proliferation by activating the Wnt/β-catenin signaling pathway. Oncol. Lett. **12**(2), 1329 (2016)
22. M. Patel, Y. Margaron, N. Fradet, Q. Yang, B. Wilkes, M. Bouvier, K. Hofmann, J.F. Côté, An evolutionarily conserved autoinhibitory molecular switch in ELMO proteins regulates rac signaling. Curr. Biol. **20**(22), 2021–2027 (2010)
23. R. Hjorten, U. Hansen, R.A. Underwood, H.E. Telfer, R.J. Fernandes, D. Krakow, E. Sebald, S. Wachsmann-Hogiu, P. Bruckner, R. Jacquet, W.J. Landis, P.H. Byers, J.M. Pace, Type XXVII collagen at the transition of cartilage to bone during skeletogenesis. Bone **41**(4), 535–542 (2007)
24. R.F. Loeser, Integrins and chondrocyte-matrix interactions in articular cartilage. Matrix Biol. **39**, 11–36 (2014)
25. Z. Liu, J. Chen, A.J. Mirando, C. Wang, M.J. Zuscik, R.J. O'Keefe, M.J. Hilton, A dual role for NOTCH signaling in joint cartilage maintenance and osteoarthritis. Sci. Signal. **8**(386), (2015)
26. K.D. Estrada, W. Wang, K.N. Retting, C.T. Chien, F.F. Elkhoury, R. Heuchel, K.M. Lyons, Smad7 regulates terminal maturation of chondrocytes in the growth plate. Dev. Biol. **382**(2), 375–384 (2013)
27. K.A. Geister, A.J. Lopez-Jimenez, S. Houghtaling, T.H. Ho, R. Vanacore, D.R. Beier, Loss of function of Colgalt1 disrupts collagen post-translational modification and causes musculoskeletal defects. DMM Dis. Model. Mech. **12**(6), (2019)
28. C. Matta, R. Zakany, Calcium signalling in chondrogenesis: implications for cartilage repair. Front. Biosci. Sch. **5**, 305–324 (2013)

29. A.D. Murdoch, T.E. Hardingham, D.R. Eyre, R.J. Fernandes, The development of a mature collagen network in cartilage from human bone marrow stem cells in Transwell culture. Matrix Biol. **15**, 16–26 (2016)
30. H.L. Ansorge, X. Meng, G. Zhang, G. Veit, M. Sun, J.F. Klement, D.P. Beason, L.J. Soslowsky, M. Koch, D.E. Birk, Type XIV collagen regulates fibrillogenesis: premature collagen fibril growth and tissue dysfunction in null mice. J. Biol. Chem. **284**(13), 8427–8438 (2009)
31. M.A. Szychlinska, G. Calabrese, S. Ravalli, N.L. Parrinello, S. Forte, P. Castrogiovanni, E. Pricoco, R. Imbesi, S. Castorina, R. Leonardi, M. Di Rosa, G. Musumeci, Cycloastragenol as an exogenous enhancer of chondrogenic differentiation of human adipose-derived mesenchymal stem cells. A morphological study. Cells **9**(2), 347 (2020)
32. D. Eyre, Collagen of articular cartilage. Arthritis Res. **4**(1), 30–35 (2002)
33. P. Smeriglio, J. Lee, N. Bhutani, Soluble Collagen VI treatment enhances mesenchymal stem cells expansion for engineering cartilage. Bioeng. Transl. Med. **2**(3), 278–284 (2017)
34. E.R. Garvican, A. Vaughan-Thomas, C. Redmond, P.D. Clegg, MT3-MMP (MMP-16) is downregulated by in vitro cytokine stimulation of cartilage, but unaltered in naturally occurring equine osteoarthritis and osteochondrosis. Connect. Tissue Res. **49**(2), 62–67 (2008)
35. A. Sharma, G. Desando, M. Petretta, S. Chawla, I. Bartolotti, C. Manferdini, F. Paolella, E. Gabusi, D. Trucco, S. Ghosh, G. Lisignoli, Investigating the role of sustained calcium release in silk-gelatin-based three-dimensional bioprinted constructs for enhancing the osteogenic differentiation of human bone marrow derived mesenchymal stromal cells. ACS Biomater. Sci. Eng. **5**(3), 1518–1533 (2019)
36. J. Chakraborty, S. Ghosh, Cellular proliferation, self-assembly, and modulation of signaling pathways in silk fibroin gelatin-based 3D bioprinted constructs. ACS Appl. Biol. Mater. **3**(12), 8309–8320 (2020)
37. F. Djouad, B. Delorme, M. Maurice, C. Bony, F. Apparailly, P. Louis-Plence, F. Canovas, P. Charbord, D. Noël, C. Jorgensen, Microenvironmental changes during differentiation of mesenchymal stem cells towards chondrocytes. Arthritis Res. Ther. **9**(2), R33 (2007)
38. M. Bhattacharjee, S. Chawla, S. Chameettachal, S. Murab, N.S. Bhavesh, S. Ghosh, Role of chondroitin sulphate tethered silk scaffold in cartilaginous disc tissue regeneration. Biomed. Mater. **11**(2), (2016)
39. S. Zhu, H. Liu, Y. Wu, B.C. Heng, P. Chen, H. Liu, H.W. Ouyang, Prevalence of methotrexate intolerance in rheumatoid arthritis and psoriatic arthritis. Arthritis Res. Ther. **15**(4), 217 (2013)
40. A. Ray, P.N.P. Singh, M.L. Sohaskey, R.M. Harland, A. Bandyopadhyay, Precise spatial restriction of BMP signaling is essential for articular cartilage differentiation. Dev. **142**(6), 1169–1179 (2015)
41. D. Studer, C. Millan, E. Öztürk, K. Maniura-Weber, M. Zenobi-Wong, Molecular and biophysical mechanisms regulating hypertrophic differentiation in chondrocytes and mesenchymal stem cells. Eur. Cells Mater. **24**, 118–135 (2012)
42. E. Mariani, L. Pulsatelli, A. Facchini, Signaling pathways in cartilage repair. Int. J. Mol. Sci. **15**(5), 8667–8698 (2014)
43. A. Wei, B. Shen, L.A. Williams, D. Bhargav, T. Gulati, Z. Fang, S. Pathmanandavel, A.D. Diwan, Expression of growth differentiation factor 6 in the human developing fetal spine retreats from vertebral ossifying regions and is restricted to cartilaginous tissues. J. Orthop. Res. **34**(2), 279–289 (2016)
44. D. Ramos, M. S. Peach, A. D. Mazzocca, X. Yu, and S. G. Kumbar: in *Regen. Eng. Musculoskelet. Tissues Interfaces.*195–217, (2015).
45. C.B. Foldager, W.S. Toh, B.B. Christensen, M. Lind, A.H. Gomoll, M. Spector, Collagen type IV and laminin expressions during cartilage repair and in late clinically failed repair tissues from human subjects. Cartilage. **7**(1), 52–61 (2016)
46. A. Muona, L. Eklund, T. Väisänen, T. Pihlajaniemi, Developmentally regulated expression of type XV collagen correlates with abnormalities in Col15a1-/- mice. Matrix Biol. **21**(1), 89–102 (2002)
47. N. Matsuo, S. Tanaka, H. Yoshioka, M. Koch, M.K. Gordon, F. Ramirez, Collagen XXIV (Col24a1) gene expression is a specific marker of osteoblast differentiation and bone formation. Connect. Tissue Res. **49**(2), 68–75 (2008)
48. X. Yang, L. Chen, X. Xu, C. Li, C. Huang, C.X. Deng, TGF-β/Smad3 signals repress chondrocyte hypertrophic differentiation and are required for maintaining articular cartilage. J. Cell Biol. **153**(1), 35–46 (2001)
49. M.B. Mueller, M. Fischer, J. Zellner, A. Berner, T. Dienstknecht, L. Prantl, R. Kujat, M. Nerlich, R.S. Tuan, P. Angele, Hypertrophy in mesenchymal stem cell chondrogenesis: effect of TGF-β isoforms and chondrogenic conditioning. Cells Tissues Organs **192**(3), 158 (2010)
50. M.B. Mueller, R.S. Tuan, Functional characterization of hypertrophy in chondrogenesis of human mesenchymal stem cells. Arthritis Rheum. **58**(5), 1377 (2008)
51. G. Zhen, C. Wen, X. Jia, Y. Li, J.L. Crane, S.C. Mears, F.B. Askin, F.J. Frassica, W. Chang, J. Yao, J.A. Carrino, A. Cosgarea, D. Artemov, Q. Chen, Z. Zhao, X. Zhou, L. Riley, P. Sponseller, M. Wan, W.W. Lu, X. Cao, Inhibition of TGF-β signaling in mesenchymal stem cells of subchondral bone attenuates osteoarthritis. Nat. Med. **19**(6), 704–712 (2013)
52. R.L. Miclea, M. Karperien, C.A.J. Bosch, G. Van Der Horst, M.A. Van Der Valk, T. Kobayashi, H.M. Kronenberg, G. Rawadi, P. Akçakaya, C.W.G.M. Löwik, R. Fodde, J.M. Wit, E.C. Robanus-Maandag, Adenomatous polyposis coli-mediated control of β-catenin is essential for both chondrogenic and osteogenic differentiation of skeletal precursors. BMC Dev. Biol. **9**, 26 (2009)

53. J. Kokavec, T. Zikmund, F. Savvulidi, V. Kulvait, W. Edelmann, A.I. Skoultchi, T. Stopka, The ISWI ATPase Smarca5 (Snf2h) is required for proliferation and differentiation of hematopoietic stem and progenitor cells. Stem Cells **35**(6), 1614–1623 (2017)
54. R.A. Oldershaw, T.E. Hardingham, Notch signaling during chondrogenesis of human bone marrow stem cells. Bone **46**(2), 286–293 (2010)
55. E.N. Blaney Davidson, E.L. Vitters, W.B. van den Berg, P.M. van der Kraan, TGF β-induced cartilage repair is maintained but fibrosis is blocked in the presence of Smad7. Arthritis Res. Ther. **8**(3), R65 (2006)
56. S. Chawla, M.H.M. Berkelaar, B. Dasen, C. Halleux, S. Guth-Gundel, I. Kramer, S. Ghosh, I. Martin, A. Barbero, P. Occhetta, Blockage of bone morphogenetic protein signalling counteracts hypertrophy in a human osteoarthritic micro-cartilage model. J. Cell Sci. **133**(23), (2020)
57. J. Hu, J. Lu, G. Lian, J. Zhang, J.L. Hecht, V.L. Sheen, Filamin B regulates chondrocyte proliferation and differentiation through Cdk1 signaling. PLoS ONE **9**(2), (2014)
58. W. Wang, D. Rigueur, K.M. Lyons, TGFβ signaling in cartilage development and maintenance. Birth Defects Res Part C Embryo Today Rev **102**(1), 37–51 (2014)
59. W. Wang, H. Chun, J. Baek, J.E. Sadik, A. Shirazyan, P. Razavi, N. Lopez, K.M. Lyons, The TGFβ type i receptor TGFβRI functions as an inhibitor of BMP signaling in cartilage. Proc. Natl. Acad. Sci. U. S. A. **116**(31), 15570–15579 (2019)
60. C. Lian, X. Wang, X. Qiu, Z. Wu, B. Gao, L. Liu, G. Liang, H. Zhou, X. Yang, Y. Peng, A. Liang, C. Xu, D. Huang, P. Su, Collagen type II suppresses articular chondrocyte hypertrophy and osteoarthritis progression by promoting integrin β1-SMAD1 interaction. Bone Res. **7**, 8 (2019)
61. R. Wilson, J.M. Whitelock, J.F. Bateman, Proteomics makes progress in cartilage and arthritis research. Matrix Biol. **28**(3), 121–128 (2009)
62. M.C. Schneider, C.A. Barnes, S.J. Bryant, Characterization of the chondrocyte secretome in photoclickable poly(ethylene glycol) hydrogels. Biotechnol. Bioeng. **114**(9), 2096–2108 (2017)
63. O.F.W. Gardner, N. Fahy, M. Alini, M.J. Stoddart, Differences in human mesenchymal stem cell secretomes during chondrogenic induction. Eur. Cells Mater. **31**, 221–235 (2016)
64. Y. Wang, Y. Li, A. Khabut, S. Chubinskaya, A.J. Grodzinsky, P. Önnerfjord, Quantitative proteomics analysis of cartilage response to mechanical injury and cytokine treatment. Matrix Biol. **63**, 11–22 (2017)
65. J. Wu, W. Liu, A. Bemis, E. Wang, Y. Qiu, E.A. Morris, C.R. Flannery, Z. Yang, Comparative proteomic characterization of articular cartilage tissue from normal donors and patients with osteoarthritis. Arthritis Rheum. **56**(11), 3675–3684 (2007)
66. S. Chameettachal, S. Midha, S. Ghosh, Regulation of chondrogenesis and hypertrophy in silk fibroin-gelatin-based 3D bioprinted constructs. ACS Biomater. Sci. Eng. **2**(9), 1450–1463 (2016)
67. S. Murab, J. Samal, A. Shrivastava, A.R. Ray, A. Pandit, S. Ghosh, Glucosamine loaded injectable silk-in-silk integrated system modulate mechanical properties in bovine ex-vivo degenerated intervertebral disc model. Biomaterials **55**, 64 (2015)
68. P. Admane, A.C. Gupta, P. Jois, S. Roy, C. Chandrasekharan Lakshmanan, G. Kalsi, B. Bandyopadhyay, S. Ghosh, Direct 3D bioprinted full-thickness skin constructs recapitulate regulatory signaling pathways and physiology of human skin. Bioprinting. **15**, (2019)
69. C. Manferdini, N. Zini, E. Gabusi, F. Paolella, E. Lambertini, L. Penolazzi, R. Piva, G. Lisignoli, Immunoelectron microscopic localization of Collagen type XV during human mesenchymal stem cells mineralization. Connect. Tissue Res. **59**, 42–45 (2018)
70. T. Glatter, C. Ludwig, E. Ahrné, R. Aebersold, A.J.R. Heck, A. Schmidt, Large-scale quantitative assessment of different in-solution protein digestion protocols reveals superior cleavage efficiency of tandem Lys-C/trypsin proteolysis over trypsin digestion. J. Proteome Res. **11**(11), 5145–5156 (2012)
71. M.F. Hsueh, A. Khabut, S. Kjellström, P. Önnerfjord, V.B. Kraus, Elucidating the molecular composition of cartilage by proteomics. J. Proteome Res. **15**(2), 374–388 (2016)
72. J. Cox, M.Y. Hein, C.A. Luber, I. Paron, N. Nagaraj, M. Mann, Accurate proteome-wide label-free quantification by delayed normalization and maximal peptide ratio extraction, termed MaxLFQ. Mol. Cell. Proteomics **13**(9), 2513–2526 (2014)